Video Article

Production of Single Tracks of Ti-6Al-4V by Directed Energy Deposition to Determine the Layer Thickness for Multilayer Deposition

Abdollah Saboori[1], Simona Tusacciu[2], Mattia Busatto[2], Manuel Lai[2], Sara Biamino[1], Paolo Fino[1], Mariangela Lombardi[1]

[1]Department of Applied Science and Technology, Politecnico di Torino

[2]IRIS S.r.l.

Correspondence to: Abdollah Saboori at abdollah.saboori@polito.it

URL: https://www.jove.com/video/56966
DOI: doi:10.3791/56966

Keywords: Engineering, Issue 133, Directed Energy Deposition, Ti-6Al-4V, Melt pool, Single track, Scanning speed, Laser power

Date Published: 3/13/2018

Citation: Saboori, A., Tusacciu, S., Busatto, M., Lai, M., Biamino, S., Fino, P., Lombardi, M. Production of Single Tracks of Ti-6Al-4V by Directed Energy Deposition to Determine the Layer Thickness for Multilayer Deposition. *J. Vis. Exp.* (133), e56966, doi:10.3791/56966 (2018).

Abstract

Directed Energy Deposition (DED), which is an additive manufacturing technique, involves the creation of a molten pool with a laser beam where metal powder is injected as particles. In general, this technique is employed to either fabricate or repair different components. In this technique, the final characteristics are affected by many factors. Indeed, one of the main tasks in building components by DED is the optimization of process parameters (such as laser power, laser speed, focus, *etc.*) which is usually carried out through an extensive experimental investigation. However, this sort of experiment is extremely lengthy and costly. Thus, in order to accelerate the optimization process, an investigation was conducted to develop a method based on the melt pool characterizations. In fact, in these experiments, single tracks of Ti-6Al-4V were deposited by a DED process with multiple combinations of laser power and laser speed. Surface morphology and dimensions of single tracks were analyzed, and geometrical characteristics of melt pools were evaluated after polishing and etching the cross-sections. Helpful information regarding the selection of optimal process parameters can be achieved by examining the melt pool features. These experiments are being extended to characterize the larger blocks with multiple layers. Indeed, this manuscript describes how it would be possible to quickly determine the layer thickness for the massive deposition, and avoid over or under-deposition according to the calculated energy density of the optimum parameters. Apart from the over or under-deposition, time and materials saving are the other great advantages of this approach in which the deposition of multilayer components can be started without any parameter optimization in terms of layer thickness.

Video Link

The video component of this article can be found at https://www.jove.com/video/56966/

Introduction

Ti-6Al-4V is the most commonly used Ti alloy in the aerospace, aircraft, automotive, and biomedical industries because of its high strength-to-weight ratio, excellent fracture toughness, low specific gravity, excellent corrosion resistance, and heat treatability. However, its further developments in other applications are challenging, owing to its low thermal conductivity and high reactivity features, which result in its poor machinability. Moreover, due to the heat hardening phenomena during the cutting, a specific heat treatment must be undertaken[1,2,3,4].

Nonetheless, additive manufacturing (AM) technologies showed great potential to be used as new manufacturing techniques that can reduce the price and energy consumption, and address some of the current challenges in the fabrication of Ti-6Al-4V alloy.

Additive manufacturing techniques are known as innovative and can fabricate a near net shape component in a layer-by-layer fashion. A layer-by-layer additive manufacturing approach, which slices a Computer Aided Design (CAD) model into thin layers and then builds the component layer by layer, is fundamental for all AM methods. In general, additive manufacturing of metallic materials can be divided into four different processes: powder bed, powder feed (blown powder), wire feed, and other routes[3,5,6].

Directed Energy Deposition (DED) is a class of additive manufacturing and is a blown powder process that fabricates three-dimensional (3D) near net shape solid parts from a CAD file similar to other AM methods. In contrast with other techniques, DED can not only be used as a manufacturing method, but also can be employed as a repairing technique for high value parts. In the DED process, metallic powder or wire material is fed by a carrier gas or motors into the melt pool, which is generated by the laser beam on either the substrate or previously deposited layer. The DED process is a promising advanced manufacturing process that is capable of decreasing the buy-to-fly ratio, and also is capable of repairing high value parts that previously were prohibitively expensive to replace or irreparable[7].

In order to achieve the desired geometric dimensions and material properties, it is vital to establish appropriate parameters[8]. Several studies have been undertaken to elucidate the relationship between the process parameters and the final properties of the deposited sample. Peyre *et al.*[9] built some thin walls with different process parameters, and then characterized them by using 2D and 3D profilometry. They showed that

Copyright © 2018 Journal of Visualized Experiments

layer thickness and melt pool volume affect the roughness parameters noticeably. Vim *et al.*[10] proposed a model in order to analyze the relation between the process parameters and geometrical characteristics of a single cladding layer (clad height, clad width, and depth of penetration).

To date, several studies on DED of Ti alloys have been reported, most of which focused on the influence of the combination of parameters on properties of massive samples[11,12,4]. Rasheedat *et al.* studied the effect of scan speed and powder flow rate on the resulting properties of the laser metal deposited Ti-6Al-4V alloy. They found that by increasing the scan speed and powder flow rate the microstructure changed from Widmanstätten to a martensitic microstructure, which results in an increment of surface roughness and the microhardness of deposited specimens[7]. Nevertheless, less attention has been paid to designing the layer thickness setting. Choi *et al.* have investigated the correlation between the layer thickness and process parameters. They have found that the main sources of error between the present height and the actual height are the powder mass flow rate and layer thickness setting[13]. Their studies did not properly implement layer thickness setting because they involved lengthy and inaccurate processes in the layer thickness setting. Ruan *et al.* have investigated the effect of laser scanning speed on the deposited layer height at a constant laser power and powder feeding rate[14]. They have proposed some empirical models for layer thickness setting which were obtained under specific processing conditions, and thus the layer thickness setting may not be precise due to the utilization of specific process parameters[15]. In contrast to previous works, the layer thickness setting process proposed in this manuscript is a rapid method which can be performed without wasting time and materials.

The main focus of this work is to develop a rapid method for the determination of layer thickness based on the characteristics of the single tracks of the Ti-6Al-4V alloy at optimum DED process parameters. Thereafter, the optimal process parameters are employed to determine a layer thickness and fabricate high-density Ti-6Al-4V blocks without wasting time and materials.

Protocol

1. Powder Characterization

1. Put 3 g of starting Ti-6Al-4V powders on a double-sided sticky carbon tape, which is located on an aluminum pin stub, and insert inside the specimen chamber of a Field-Emission Scanning Electron Microscope (FESEM) to analyze the morphology of the powder[16].
2. Measure the apparent density of the powder by filling a 30 cm^3 container, and measure the weight of powder according to the ASTM-B212 standard.
3. Perform chemical analysis of starting powder (5 - 10 g), used powder (5 - 10 g), and deposited block (20 g) by means of elemental (*e.g.*, Leco) and inductively coupled plasma (ICP) analyzer[17].

2. Directed Energy Deposition of Single Tracks

1. **Powder Loading**
    1. Wear personal protective equipment, including an FFP3 respiratory mask compliant to the requirements of EN 149, powder-free disposable nitrile gloves, and protective plastic glasses.
    2. Open the hopper of the powder feeding system and use an extractor fan (*e.g.*, ATEX) for removing the residual powders.
    3. Remove the hopper by following the appropriate instructions given by the constructor and clean every component by using ethanol-soaked paper towels.
    NOTE: This step is fundamental to avoid contamination by different kinds of metal powders.
    4. Reassemble the powder feeding hopper by following the instructions given by the constructor. Leave aside only the top cap of the hopper in order to perform the loading of the powder.
    5. Load the hopper with Ti-6Al-4V powders having granulometry in the range of 50 - 150 µm. Depending on the size of the available hopper, fill it completely.
    6. Close the top cap of the hopper very tightly in order to avoid any gas leakage.

2. **Preparation of the Sample**
    1. Pick a Ti-6Al-4V sheet with 50 mm x 50 mm dimensions and 4 mm thickness.
    2. Clean the surface of the titanium sheet with ethanol-soaked paper towels. Measure the weight of the sheet with a centesimal balance.
    3. Place the sheet on the working area according to the position of the marker. The working area is where the deposition will take place, so it is determined according to the programmed path of the robot.

3. **Preparation of the Robot and Preparation of the Deposition Equipment**
    1. Mount the nozzle on the laser head so that the angle between the nozzle axis and the laser axis is 35°.
    2. Move the robot to the starting working point to perform the calibration.
    3. Check the distance between the nozzle and the working plane and, if needed, manually correct the nozzle position until the measured distance is 5 mm.
    NOTE: Since the working area lays on a horizontal plane, this distance is the vertical distance between the metal sheet and the tip of the nozzle.
    4. Check the centering of the nozzle outlet with the laser: first, switch on the laser guide by clicking the "Laser Guide ON" command on the software for the control of the laser. Then, put a thin rod, measuring 0.8 mm in diameter and 200 mm in length, inside the nozzle. Verify that the tip of the rod and the spot of the laser guide are coincident. If not, manually adjust the position of the nozzle, respecting the distances and angles previously indicated.
    NOTE: In this case, the outer diameter of the nozzle is 1 mm; if a nozzle with a smaller diameter is employed, use a rod whose diameter is smaller than that of the nozzle.
    5. Verify the calibration data written into the robot control software: click the button "Apply" on the software, and wait for the compilation of the code.

NOTE: The software will check for errors in the code; if no errors are detected, the code is stored on the robot controller. If errors are detected, the code won't be compiled, and further revision will be needed.

6. Enable the laser source module by clicking the "Laser enable" command on the laser control software.
   NOTE: The employed laser source is a continuous fiber laser emitting in the infrared region (1064 nm) with 5 kW maximum power.
7. Enable the robot's motors by manually pushing the button "Robot Motors on" on the control cabinet of the robot, and check that the related safety LED is lit up: if so, it means that the motors are enabled.

4. **Start the Deposition Process**
   1. Select the proper file on the existing program list and load the working path into the main robot routine.
   2. Check the laser and robot parameters: set the laser power to the specific laser power (325, 650, 980, 1500 W) and the robot speed to a given speed (30, 40, 50, 60 mm/s).
      NOTE: These parameters are written into the control software of the robot, according to the specific language of the machine.
   3. Confirm the new parameters by pushing the button "Apply" on the software, and wait for the compilation of the code. The software will check for errors in the code; if no errors are detected, the code is stored on the robot controller and it is ready to be launched. Launch the robot routine by pushing the "START" button on the robot control software.

5. Pick up the sample by using the special nipper, and clean the sample surface with an ethanol-soaked paper towel for removing any residual powder.

3. Analyze the Single Tracks

1. Analyze the single tracks from the top by a stereo microscope at 5X magnification.
   NOTE: In this stage, some images are taken by means of a stereo microscope and analyzed visually.
2. Cut the single tracks from the middle of the deposited tracks perpendicular to the deposition direction by using a precise cutting tool.
3. Mount the cross section of single tracks in epoxy resin. Choose a mounting cup and place the clean and dry specimen in it. Measure the correct amounts of resin carefully by weight (10 g/sample) and then mix with a liquid hardener (6 g/sample). Pour the resin-mixture over the specimen and leave the filled mounting cups to cure for 30 min at room temperature. Thereafter, grind the mounted specimens with 500, 800, and 1,200 grit size SiC paper, and then polish by using diamond paste down to the finer sizes of diamond particles (1 µm).
4. Analyze the polished surfaces in terms of shape and porosity by means of an optical microscope. Acquire the images of melt pools with the optical microscope at 10X magnification, and then analyze them using Image-J software.
5. Measure the height of melt pools by measuring the distance between the top and bottom of the melt pool. Afterwards, plot the measured height of melt pools as a function of specific energy density, which is calculated according to its corresponding equation. Indeed, the energy density can be calculated by the following equation:
   $$E = \frac{p}{vD}$$
6. Fit a 2nd order polynomial on the experimental results to obtain the equation corresponding to the layer thickness as a function of specific energy density.
7. Consider a specific energy density, and calculate the layer thickness according to their relationship, which was observed in the previous step.
8. To verify the method, fabricate a multilayer block by considering the calculated layer thickness, and then characterize the section of blocks in terms of porosity and final height.
9. Analyze the microstructure of the fabricated block after a polishing step in the same procedure as section 3.3. In fact, after final polishing, etch the samples for 30 s with Kroll's Reagent, which contains 92 mL distilled water, 6 mL nitric acid, and 2 mL hydrofluoric acid.

Representative Results

For the experimental studies, irregular Ti-6Al-4V powder with an average size of 50 - 150 µm and apparent density of 1.85 g/cm^3 was employed as depositing material (**Figure 1**). The chemical analysis of the powder confirmed that the oxygen and nitrogen contents of the powder did not change before and after the deposition process, while in both cases the oxygen content was higher than the standard oxygen content of Ti-6Al-4V powder for additive manufacturing (<0.13%). However, the oxygen and nitrogen content of the bulk components increased after the deposition.

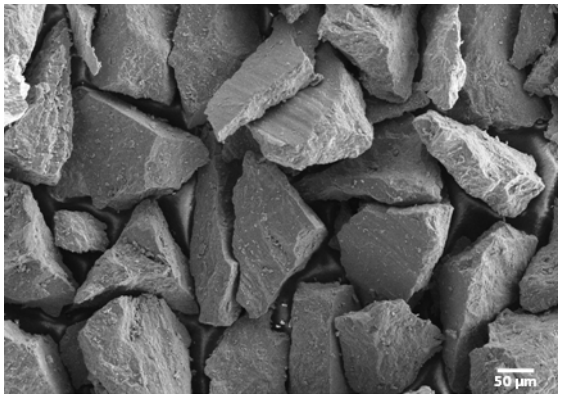

Figure 1: Starting Ti-6Al-4V powder is used as depositing material. This is an irregular powder with an average size of 100 - 150 µm and apparent density of 1.85 g/cm^3.

	C	S	Al	Fe	H	N	O	V	Ti
Fresh powder	0.017	<0.001	5.83	0.08	0.013	0.022	0.23	3.89	Bal.
Used Powder	0.016	<0.001	5.86	0.08	0.012	0.02	0.22	3.87	Bal.
Bulk component	0.021	0.001	5.78	0.08	0.012	0.058	0.28	3.8	Bal.
Standard	< 0.08	--	5.5-6.5	<0.25	<0.012	<0.05	<0.13	3.5-4.5	Bal.

Table 1: The chemical composition of Ti-6Al-4V powder before and after deposition (weight percentage). It shows that the oxygen and nitrogen contents of the powder do not change before and after the deposition process, while in both cases the oxygen content is higher than the standard oxygen content of Ti-6Al-4V powder for additive manufacturing.

Figure 2 shows the single tracks of the Ti-6Al-4V alloy after deposition at various laser power and laser scan speed. As can be seen by increasing the laser power and decreasing the laser scan speed, the size of single tracks increased.

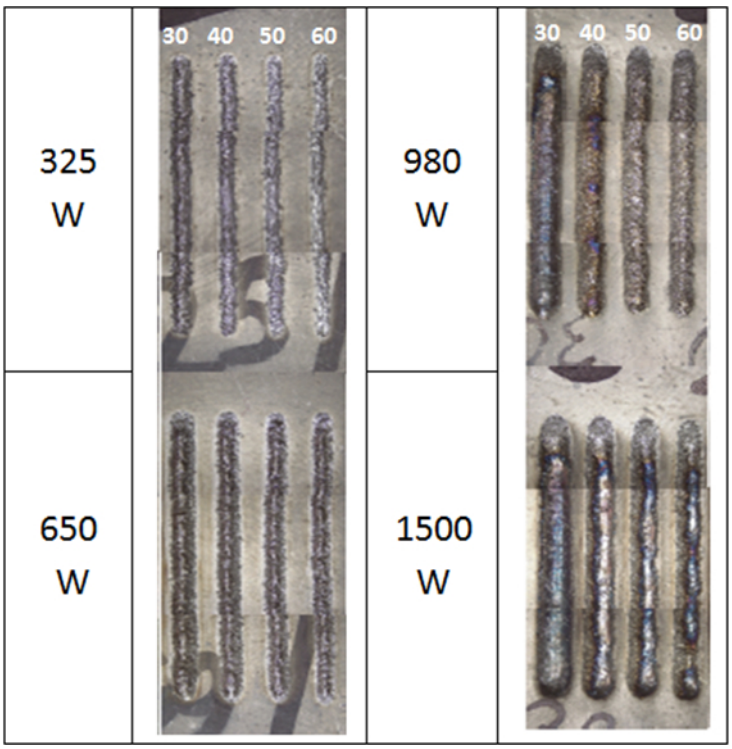

Figure 2: Single tracks of the Ti-6Al-4V alloy after deposition. These single tracks were deposited at different laser power and laser scan speed and analyzed from the top. By increasing the laser power and decreasing the laser scan speed, their sizes increased.

Figure 3 shows the cross section of single tracks after the deposition, and by increasing the laser power, the height of single tracks increased considerably. Moreover, by decreasing the laser scan speed at a constant laser power, the height of deposition increased while, at low laser power and very high laser scan speed, the height of deposition was negligible. Despite the height of the melt pool, the porosity formation inside the melt pool, in particular near the interface of the melt pool/fusion zone area, was another phenomenon which was revealed after the deposition.

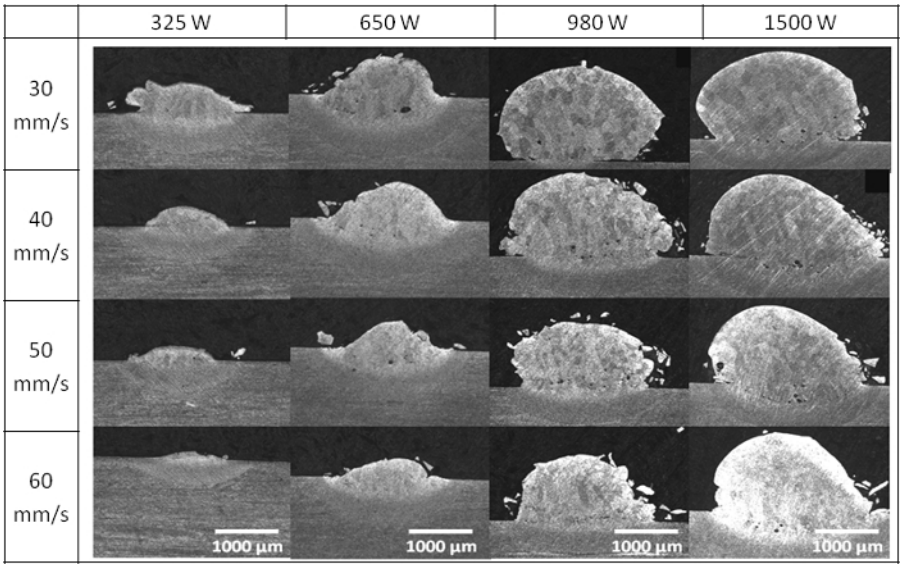

Figure 3: Cross section of single tracks after the deposition. By increasing the laser power and decreasing the laser scan speed, the height of melt pool decreased. Please click here to view a larger version of this figure.

The relationship between the single track height and different process parameter is shown in **Figure 4**. The height of single tracks at different laser scan speeds increased by increasing the laser power, which suggests that the laser power up to a certain point has a positive effect on the deposition height (**Figure 4a**). However, after that critical point, the laser power negatively affects the growth of deposition due to the delivery of too much energy into the melt pool. Furthermore, it was found that as the laser scanning speed increased, the energy input in the melting pool was reduced and the powder delivery rate was indirectly decreased, and consequently the deposited height decreased remarkably (**Figure 4b**).

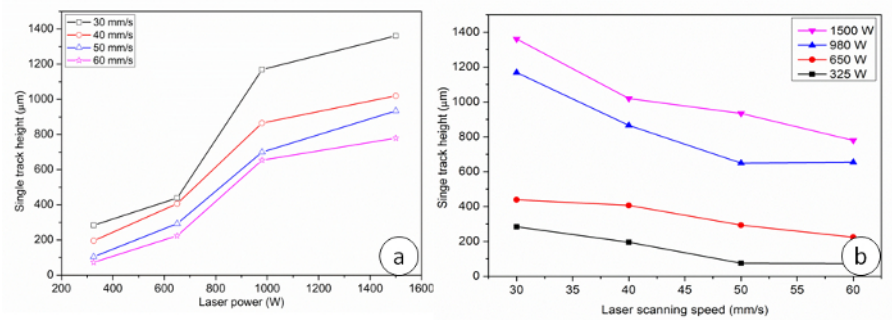

Figure 4: Effect of different process parameters on single track dimension. It is clear that as the laser scanning speed increased **(b)**, the energy input in the melting pool is reduced and the powder delivery rate **(a)** is indirectly decreased and, consequently, the deposited height decreased remarkably. Please click here to view a larger version of this figure.

These results clearly demonstrate the influence of different process parameters on the geometry of deposited tracks. Despite providing valuable insight into the process, the assessment of the deposited height is still challenging, due to the variety of parameters which were involved. Thus, some efforts have been undertaken to develop a new strategy to evaluate the effect of the combination of process parameters on the geometry of deposited track.

As was shown, the height of deposited layer increased by increasing the laser power, and it was understood that this was not the only parameter that affects the height of the melting pool. In fact, in the period of time needed to melt a given volume of the substrate and deposit an appropriate layer of molten material, a certain amount of energy and powder should be provided to the substrate. This energy is not only determined by laser power and laser scan speed, but also the laser spot size should be considered. For this purpose, the specific energy density per unit spot size (E) and powder feed density (F) is calculated to evaluate the effect of the combination of these parameters.

E, which is the specific energy density, shows the energy that is delivered into the melt pool by the laser, and in principle is responsible for melting the substrate and powder. This energy density is expressed as[8]

$$E = \frac{p}{vD} \quad (1)$$

Where *E* is the specific energy density per unit spot size, *P* is the laser power (*W*), *v* is the laser scan speed (mm/s), and *D* is laser spot size (mm). To obtain an appropriate deposition level for each metallic material, there is a certain level of energy below which no fusion bonds can be achieved, and beyond that the dilution becomes too large. Another factor that shows the effect of the combination of parameters is the powder density (*F*), which can be calculated as follows[8]

$$F = \frac{G}{vD} \quad (2)$$

Here, *F* is the powder feed density, and *G* is the powder feeding rate (g/s).

Figure 5 demonstrates the variation of deposited layer height as a function of specific energy density. As can be seen, the height of single tracks increased by increasing the specific energy density, which can be related to the higher heat input at the higher laser energy density. The empirical correlation between the energy density and the height of deposition are as follows:

h = 14.99 E – 17.85 (3)

From this equation, the height of deposited track can be estimated through the calculation of the specific energy density and this equation. On the other hand, the variation of deposited height as a function of powder density, which is shown in **Figure 6**, showed that by increasing the powder density, the height of deposited track increased, and the empirical relationship between these can be expressed as follows:

h = 38477 F – 157.06 (4)

This equation shows that the height of deposited track can be calculated by calculating the powder density and this equation. Eq. 3 and Eq. 4 show that by using the combination of process parameters and calculating the specific energy density and powder density, it is possible to forecast the deposited height, and consequently find the best domain to achieve the best deposition quality.

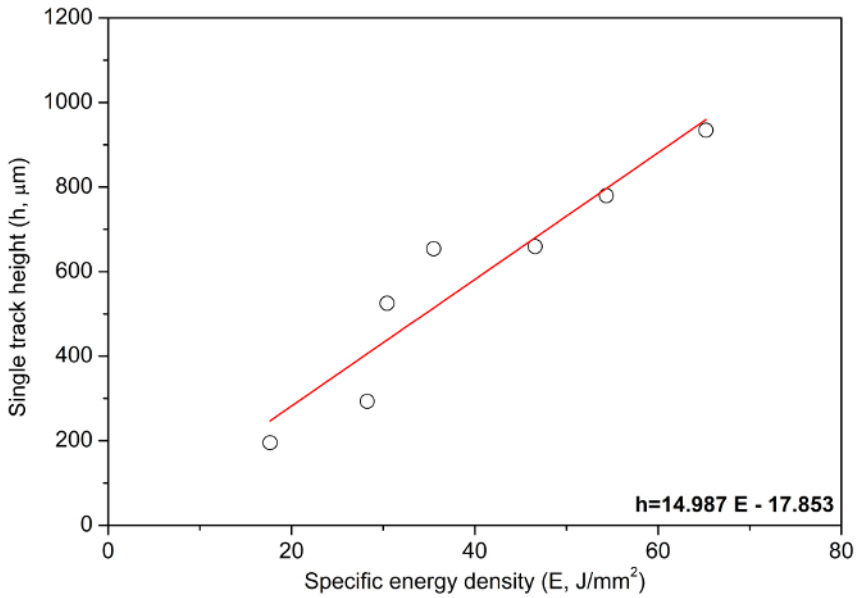

Figure 5: Single track height (h) versus specific energy density (E). The height of single tracks increased by increasing the specific energy density, which can be related to the higher heat input at higher laser energy density. Please click here to view a larger version of this figure.

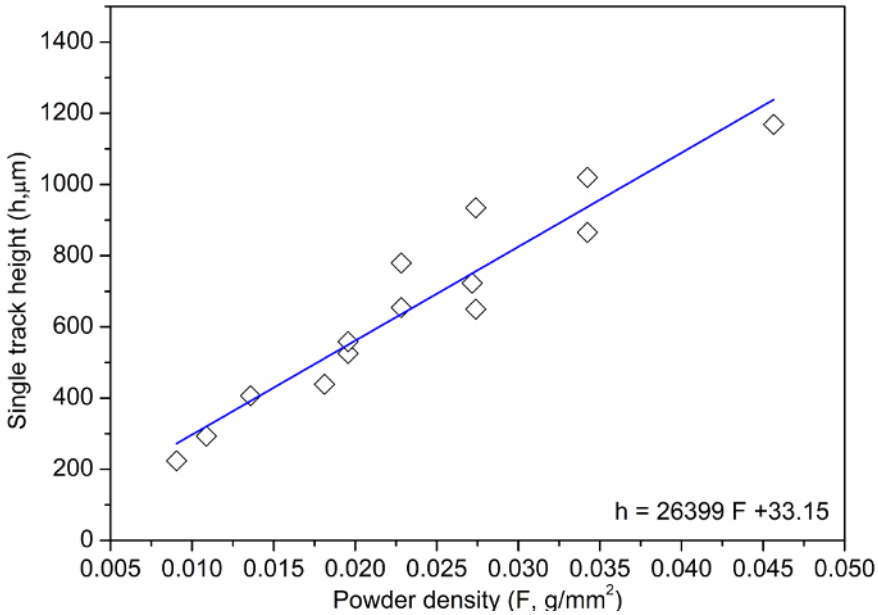

Figure 6: Single track height (h) as a function of powder feed density (F). By increasing the powder feed density, the height of deposited track increased. Please click here to view a larger version of this figure.

In direct energy deposition of metallic materials, h (the layer height, or *ΔZ*) is a very important factor that affects the quality of component after the deposition. In the conventional direct energy deposition of metallic components, the height of the deposition layer is considered a constant and, apart from the geometry of component and its material, the process parameters such laser power and laser scanning speed were optimized to fabricate the final component. Indeed, slicing the layers in a constant thickness does not usually conform to the process parameters. Therefore, this thickness may be altered either manually or empirically, which sacrifices the quality of component and the fabrication rate. In general, in conventional layer slicing, over- or under-deposition may be achieved due to the approximations in the consideration of the layer thickness, which needs further corrections such as subsequent deposition or machining the extra layers (**Figure 7a**). Thus, in this work, effort has been undertaken to develop a new strategy to determine the layer thickness, according to the process conditions which are used in the production of components.

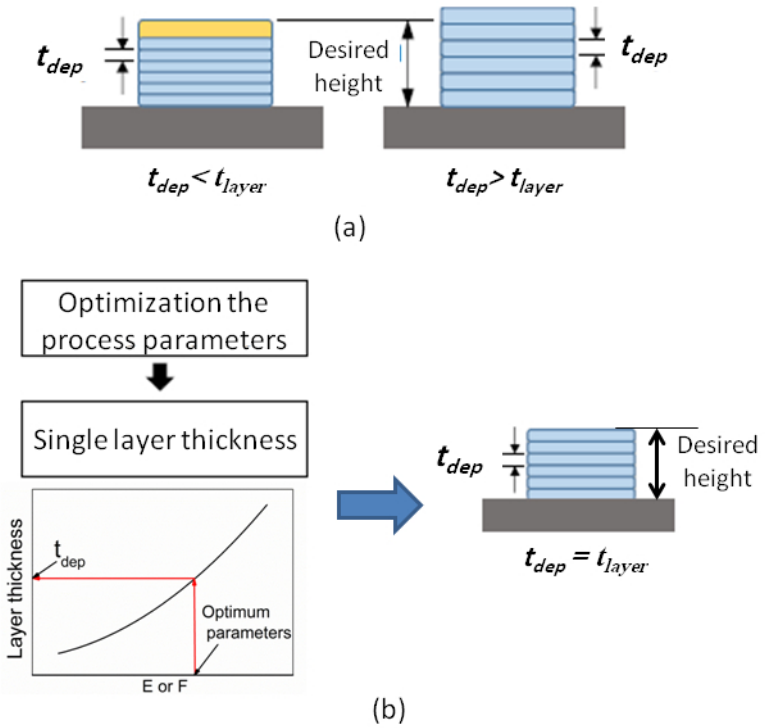

Figure 7: Slicing. (a) conventional slicing strategy, **(b)** new slicing strategy according to the optimum process parameters; in conventional layer slicing, over- or under-deposition may be achieved due to the approximations in the consideration of the layer thickness, which needs further corrections, such as subsequent deposition or machining the extra layers. In this approach, the layer thickness for the fabrication of component is determined according to a single layer height related to the specific energy density of two combined parameters. E is the specific energy density per unit spot size, F is the powder feed density, t_{dep} is the single layer thickness, and t_{layer} is the slice thickness.

In fact, in this approach, the layer thickness for the fabrication of component is determined according to a single layer height related to the specific energy density of two combined parameters. To proof this method and check the correlation between the quality of the component and different layer thickness, some simple cubes were built at various ΔZ and then their cross sections were evaluated.

Figure 8a-b show the representative cross-sections of multilayer-blocks, which were produced according to the conventional method. As can be seen in **Table 2**, according to the slicing strategy which considers 0.325 mm as the layer thickness, the desired height of the block shown in **Figure 8a** should be approximately 5.2 mm. However, in the conventional method, the final height of 10.11 mm (over-deposition) was achieved, which is a consequence of considering a high ΔZ (0.6 mm) during the process. This over-deposition process resulted in the lack of fusion between the layers, and a high level of porosity inside the specimen. On the other hand, **Figure 8b** illustrates that by considering a low ΔZ, the desired height cannot be achieved, and this results in a long deposition process and undesirable microstructure. These discrepancies imply that in the conventional method, slicing the layers in a fixed thickness does not usually conform to the process parameters, and thus the desired layer thickness cannot be achieved. A cross-section of the block, which was produced according to the slicing strategy, is shown in **Figure 9**. As can be seen through considering an appropriate ΔZ, it could be possible to achieve excellent dimensional accuracy. However, the dimensional accuracy can be decreased at a high level of laser power as a consequence of high input energy, which results in the melting of underlying layer. **Table 2** shows that by using the slicing method, a more stable melting pool position can be achieved, and consequently the dimensional accuracy increases. **Figure 9** shows a block which is produced according to the slicing approach, and as can be seen by using an appropriate ΔZ (~ 0.5 mm) the desired height of deposition was obtained.

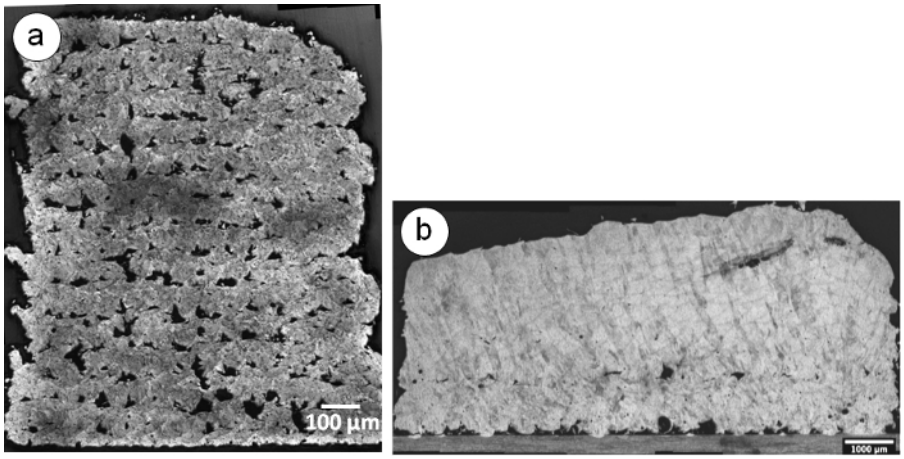

Figure 8: Examples of specimens produced by the conventional method. According to the slicing strategy which considers 0.325 mm as the layer thickness, the desired height of the block which is shown in panel **a** should be approximately 5.2 mm. However, in the conventional method, the final height of 10.11 mm (over-deposition) was achieved, which is a consequence of considering a high ΔZ (0.6 mm) during the process. On the other hand, panel **b** illustrates that by considering a low ΔZ, the desired height cannot be achieved, and results in a long deposition process and undesirable microstructure. Please click here to view a larger version of this figure.

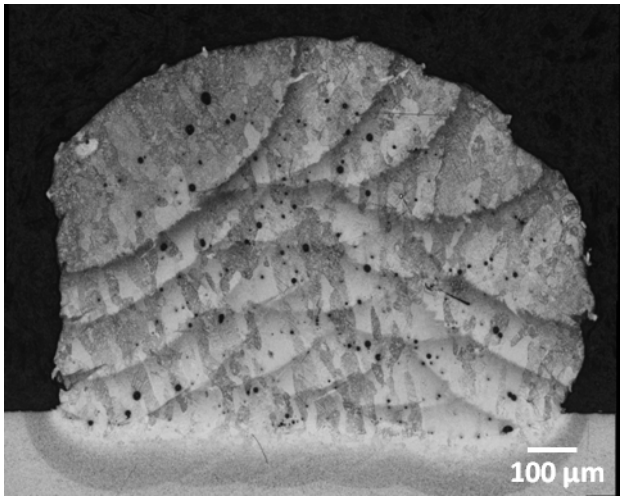

Figure 9: Example of a sample fabricated by the slicing approach. It confirms that a proper ΔZ consideration results in an excellent dimensional accuracy.

	Laser power (W)	Layer thickness (mm)	Number of layers	Desired height (mm)	Deposited height (mm)
Conventional method	350	0.325	16	5.206	10.114
	1500	0.758	8	6.07	3.425
Slicing method	325	0.485	5	7.436	7.245

Table 2: Comparison between the deposited height and desired height in conventional and slicing methods. It shows that by using the slicing method, a more stable melting pool position can be achieved and, consequently, the dimensional accuracy increases.

Discussion

In this work, the focus was on the slicing thickness setting in the DED process of Ti-6Al-4V, according to the geometry of melt pool characteristics. For this purpose, a two-step protocol was defined and utilized. The first part of the protocol was an optimization of process parameters for single scan deposition and, during this step, the optimum parameters were achieved and the melt pool geometries were measured. In the second part of the protocol, the specific energy density of specimens at the optimum parameters was calculated. In this step, the height of the melt pool was plotted as a function of energy density and, in this critical step, the layer thickness for the multilayer deposition can be achieved.

In DED, since various process parameters alter the thickness of layers, the deposition of layers with a constant layer thickness cannot result in a precise geometry of the component. It means that considering a fixed layer thickness for deposition, regardless of process parameters, leads to under- or over-deposition that results in geometric error and, consequently, a long production process. The purpose of this investigation was to explore the relationship between the slicing thickness setting procedure, the actual deposited height, and the process conditions. It was

concluded that through the combination of the geometry of the melt pool and process parameters, it would be possible to determine the optimum layer thickness associated with the specific process parameters in a shorter period of time with respect to the traditional methods.

The slicing strategy uses the equations that obtain the single-layer height related to the specific energy density. The final component is sliced according to the single layer height for a specific depositing condition. In order to verify the suggested method, some blocks were produced according to the slicing approach. The results of this research have shown that by employing this protocol, it would be possible to determine the layer thickness, which is one of the main parameters that should be considered correctly to build a component with accurate dimensions. The only limitation of this protocol that may be considered is the dependence of the outcomes on the type of material, and thus this protocol should be undertaken for every type of material. In addition, to increase the accuracy of the layer thickness setting, the width of the melt pool can also be considered in the protocol. The most important step in the protocol is the measurement of the melt pool geometry so that any error, even small errors, in this step may result in a significant error in the layer thickness setting.

Disclosures

The authors have nothing to disclose.

Acknowledgements

The authors would like to acknowledge the European research project belonging to the Horizon 2020 research and innovation program Borealis - the 3A energy class Flexible Machine for the new Additive and Subtractive Manufacturing on next generation of complex 3D metal parts

References

1. Banerjee, D., Williams, J.C. Perspectives on Titanium Science and Technology. *Acta Mater.* **61**(3):844-879 (2013).
2. Peters, M. *Titanium and Titanium Alloys Edited by.* (Leyens, C., Peters, M., eds.). WILEY-VCH Verlag GmbH & Co. KGaA (2003).
3. Lin, J., Lv, Y., Liu, Y., et al. Microstructural evolution and mechanical property of Ti-6Al-4V wall deposited by continuous plasma arc additive manufacturing without post heat treatment. *J Mech Behav Biomed Mater.* **69**(December 2016):19-29 (2017).
4. Saboori, A., Gallo, D., Biamino, S., Fino, P., Lombardi, M. An Overview of Additive Manufacturing of Titanium Components by Directed Energy Deposition: Microstructure and Mechanical Properties. *Appl Sci.* **7**(9) (2017).
5. Wu, X., Liang, J., Mei, J., Mitchell, C., Goodwin, P.S., Voice, W. Microstructures of laser-deposited Ti-6Al-4V. *Mater Des.* **25**(2):137-144 (2004).
6. Trevisan, F., Calignano, F., Aversa, A., et al. Additive manufacturing of titanium alloys in the biomedical field: processes, properties and applications. *J Appl Biomater Funct Mater.* In-Press (2017).
7. Mahamood, R.M., Akinlabi, E.T. Scanning speed and powder flow rate influence on the properties of laser metal deposition of titanium alloy. *Int J Adv Manuf Technol.* (2017).
8. Shim, D., Baek, G., Seo, J., Shin, G., Kim, K., Lee, K. Effect of layer thickness setting on deposition characteristics in direct energy deposition (DED) process. *Opt Laser Technol.* 86:69-78 (2016).
9. Gharbi, M., Peyre, P., Gorny, C., et al. Influence of various process conditions on surface finishes induced by the direct metal deposition laser technique on a Ti-6Al-4V alloy. *J Mater Process Technol.* **213**(5):791-800 (2013).
10. Davim, J.P., Oliveira, C., Cardoso, A. Predicting the geometric form of clad in laser cladding by powder using multiple regression analysis (MRA). *Mater Des.* **29**(2):554-557 (2008).
11. Kobryn, P.A., Moore, E.H., Semiatin, S.L. The Effect Of Laser Power And Traverse Speed On Microstructure, Porosity, And Build Height In Laser-Deposited Ti-6Al-4V. *Scripta Materialia.* **43**:299-305 (2000).
12. Bi, G., Gasser, A., Wissenbach, K., Drenker, A., Poprawe, R. Characterization of the process control for the direct laser metallic powder deposition. *Surf Coatings Technol.* **201**(6):2676-2683 (2006).
13. Choi, J., Chang, Y. Characteristics of laser aided direct metal/material deposition process for tool steel. *Int J Mach Tools Manuf.* **45**(4):597-607 (2005).
14. Ruan, J., Tang, L., Liou, F.W., Landers, R.G. Direct Three-Dimensional Layer Metal Deposition. *J Manuf Sci Eng.* **132**(6):64502-64506 (2010).
15. Chen, X., Tao, Z. Maximum thickness of the laser cladding. *Key Eng Mater.* **46-47**:381-386 (1989).
16. Slotwinski, J.A., Garboczi, E.J., Stutzman, P.E., Ferraris, C.F., Watson, S.S., Peltz, M.A. Characterization of Metal Powders Used for Additive Manufacturing. *J Res Natl Inst Stand Technol.* 119:460-493 (2014).
17. Manfredi, D., Calignano, F., Krishnan, M., Canali, R., Ambrosio, E.P., Atzeni, E. From Powders to Dense Metal Parts: Characterization of a Commercial AlSiMg Alloy Processed through Direct Metal Laser Sintering. *Materials (Basel).* **6**(3):856-869 (2013).

Copyright © 2018 Journal of Visualized Experiments